Biosensors and Bioelectronics 60 (2014) 195–200

Contents lists available at ScienceDirect

Biosensors and Bioelectronics

journal homepage: www.elsevier.com/locate/bios

A highly sensitive microRNA biosensor based on hybridized microRNA-guided deposition of polyaniline

Huimin Deng, Wei Shen, Yuqian Ren, Zhiqiang Gao *

Department of Chemistry, National University of Singapore, Singapore 117543, Republic of Singapore

ARTICLE INFO

Article history:
Received 14 February 2014
Received in revised form
4 April 2014
Accepted 15 April 2014
Available online 25 April 2014

Keywords:
Microrna
DNAzyme
Polyaniline
Electrochemical impedance
Gold electrode

ABSTRACT

On the basis of hybridized microRNA (miRNA)-guided deposition of polyaniline (PAn), a highly sensitive impedimetric miRNA biosensor is developed in this report. Briefly, a gold electrode coated with charge neutral peptide nucleic acid (PNA) capture probes (CPs) is first hybridized to a target miRNA. After a very brief rinsing the hybridized electrode is incubated in pH 3.0 of 0.10 M potassium phosphate buffer-based cocktail containing aniline, H_2O_2, and a G-qudraplex-hemin DNAzyme. The DNAzyme catalyzes the polymerization of aniline and the hybridized miRNA strands guide the deposition of PAn, thus resulting in the formation of a thin PAn film on the biosensor surface. Electron-transfer impeding power of the PAn film in alkaline medium is utilized to determine the concentration of the target miRNA. Under optimized experimental conditions, 0.50 fM target miRNA is successfully detected. Excellent mismatch discrimination capability of the biosensor was observed largely due to the excellent hybridization selectivity of the PNA CPs. Attempts were made in profiling miRNAs in total RNA samples extracted from cancer cells and blood.

1. Introduction

Because of the emerging diagnostic and prognostic values of miRNAs, intensive research efforts have been devoted to the development of miRNA assays for uses at point-of-care. It is of paramount importance that the method for miRNA expression profiling should be highly sensitive, selective, and only analyze mature miRNAs as they are the active form of miRNAs. Toward this goal, label-free miRNA assays represent a group of attractive candidates for miRNAs expression analysis, enabling multiplexed miRNA expression profiling with much simplified protocols and with minimal sample preparation. So far, several label-free approaches, such as Taqman probe-based fluorometry (Yin et al., 2012), silver nanorod-based SERS (Driskell and Tripp, 2010), nanomechanic atomic force microscopy (Husale et al., 2009), dynamic piezoelectric cantilever (Johnson and Mutharasan, 2012), stacking-hybridized universal tag (Duan et al., 2011; Shen et al., 2012), single-stranded DNA binding protein-assisted capillary-electrophoresis (Dodgson, et al., 2012; Wegman and Krylov, 2011), nanoparticle-based colorimetry (Zhang et al., 2009; Shen et al., 2013a), and electrochemical biosensors (Gao et al., 2013; Shen et al., 2013b) have been reported. Among them, the development of label-free electrochemical biosensors appears especially appealing, particularly electrochemical impedance spectroscopy (EIS)-based label-free biosensors. The inherent miniaturization of electrochemical biosensors and their compatibility with standard microfabrication and semiconductor technologies, coupled with high sensitivity assured by chemical/electrochemical amplification strategies, provide tremendous opportunities for the electrochemical biosensors to play a significant role in future miRNA expression analysis. Their high portability and affordability could allow miRNAs expression to be profiled in a decentralized setting such as at point-of-care. To date, several EIS approaches have been attempted in the development of miRNA biosensors. For example, based on ruthenium oxide (RuO_2) nanoparticle-initiated deposition of an insulating film, EIS detection of miRNAs can be conveniently performed after the miRNAs are tagged with RuO_2 nanoparticles. (Peng and Gao, 2011) However, RuO_2-tagging procedure is a major drawback. More recently, on the basis of catalyzed deposition of poly(3,3-dimethoxybenzidine) by horse reddish peroxidase (Gao et al. 2013) label-free EIS biosensors for miRNAs were reported. Thereafter detection limits of 2.0 fM were observed. The multistep procedure in the preparation of biosensors or in the detection of miRNAs may hinder its further development.

To further enhance the sensitivity and simplify the detection protocol, a simple and yet highly sensitive biosensor for label-free detection of miRNAs was described in this report. Through incorporating a cumulative signal amplification mechanism – the hybridized target miRNA-guided deposition of polyaniline (PAn),

* Corresponding author. Tel.: +65 163887; fax: +67 791691.
E-mail address: chmgaoz@nus.edu.sg (Z. Gao).

http://dx.doi.org/10.1016/j.bios.2014.04.023
0956-5663/

label-free detection of miRNAs was realized through measuring the charge-transfer resistance (R_{ct}) of biosensor in EIS. As compared to previous reports, the procedure was simplified and the much higher efficiency in the polymerization of aniline and the subsequent deposition of PAn resulted in a sub-femtomolar detection limit.

2. Experimental section

2.1. Materials and reagents

Cysteine-terminated PNA CPs were custom-made by Biosynthesis, Inc. (Lewisville, TX) and used as received. Synthetic let-7 miRNAs and DNAzyme were from Integrated DNA Technologies. Completely complementary PNA CPs were used for the construction of the respective miRNA biosensors. Hemin (> 98%) was purchased Sigma-Aldrich. All other chemicals of certified analytical grade were obtained from Sigma-Aldrich and used without further purification. Freshly-distilled aniline was used in the deposition of PAn. Total RNA extraction kit was purchased from Invitrogen. A pH 8.0 of 0.10 M phosphate buffer was used as the hybridization and washing buffer. A pH 3.0 of 0.10 M potassium phosphate buffer containing 50 mM aniline, 400 mM H_2O_2, and 10 μM DNAzyme was used as the PAn deposition cocktail. To eliminate the effect of RNase on the stability of RNA, all surfaces were decontaminated with RNaseZap; all vessels were autoclaved; and all solutions were treated with diethyl pyrocarbonate. The PNA CP solution used for the preparation of the biosensor was typically 2.0 μM (Briones et al., 2004).

2.2. Biosensor fabrication

A cleaned gold bead electrode with a predominant (111) faceting of the surface (Fig. S1) was incubated in 100 μL of 2.0 μM PNA solution in a sealed centrifuge tube for 4 h at room temperature. After the incubation, the electrode was washed with 1:1 (v/v) mixture of water and acetonitrile, water, respectively, and dried in a stream of Ar. The PNA CP coated electrode was further incubated in 1.0 mg/mL cysteine for 2 h during which PNA molecules realign their molecular axes with the normal surface. The surface coverage of the PNA CP monolayer, estimated electrochemically using a published procedure (Sabatani and Rubimstein, 1987), was found to be in the range of 11.8–13.5 pmol/cm^2. The biosensor was stable for at least two months when stored in a clean environment.

3. Results and discussion

3.1. Detection scheme

The principal steps in the operation of the biosensor are schematically shown in Fig. 1. A monolayer of charge neutral PNA CPs, acting as a bioaffinitive interface, is self-assembled on the surface of the gold bead electrode. To improve the quality and stability of the PNA CP monolayer and to minimize non-specific deposition of PAn, cysteine is used to fill in the defects of the PNA monolayer, forming a mixed monolayer. Incubation of the biosensor in the hybridization buffer containing the target miRNA brings the target miRNA strands together with a high density of negative charges onto the biosensor (step A). A subsequent incubation of the hybridized biosensor in a cocktail consisting of the DNAzyme, aniline, and H_2O_2 results in the oxidative polymerization of aniline catalyzed by the DNAzyme and the deposition of PAn guided by the anionic target miRNA strands hybridized to the PNA CPs. Strong electrostatic attraction between anionic miRNA strands and protonated aniline molecules produces a high concentration of protonated aniline and creates a high concentration of protons (acidity) at the biosensor surface. The high concentration of aniline and high acidity greatly facilitate the polymerization aniline and the deposition of PAn in the presence of a catalyst (the DNAzyme) and an oxidant (H_2O_2). Oxidative polymerization of aniline is catalytically initiated by the DNAzyme and the deposition of PAn is guided by the hybridized target miRNA strands at the biosensor surface (step B). The excellent electron-transfer impeding power (insulating power) of the deposited PAn in alkaline medium allows EIS detection of the target miRNA (step C). High sensitivity can be conveniently realized after a sufficiently long period of incubation in the PAn deposition cocktail. The utilization of neutral PNA instead of anionic DNA in the biosensor effectively alleviates the undesired (unrelated to miRNA hybridization) adsorption of aniline molecules and their subsequent polymerization and deposition, thus producing a minimal background and facilitating the detection of miRNA at ultralow levels.

3.2. Feasibility study

It was reported that in the presence of polyanionic templates such as nucleic acid molecules, the formation of PAn occurs exclusively along the polyanionic molecules (Ma et al., 2004). It was also reported that many G-rich DNA sequences are able to form G-quadruplexes and display peroxidase-like activities after complexing with hemin, known as DNAzyme (Travascio et al., 1998). Similar to HRP, DNAzyme is capable of initiating the polymerization and subsequent deposition of PAn guided by

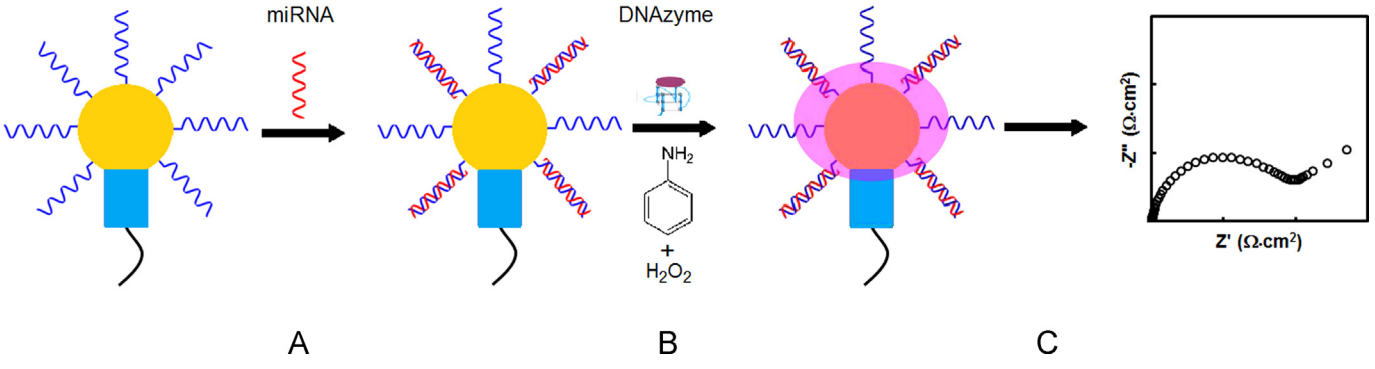

Fig. 1. Schematic illustration of the working principle of the label-free miRNA biosensor. (A) miRNA hybridization, (B) hybridized miRNA-guided PAn deposition, and (C) EIS measurement.

prefabricated DNA nanostructures (Wang et al., 2013). The time-dependent study of the deposition of PAn indicated that the growth of PAn occurs exclusively along the DNA templates (Wang et al., 2013). On the other hand, it sounds a bit peculiar that PAn is utilized to create an electron-impeding layer on the biosensor surface since being a well-studied conducting polymer PAn is best known for its electron-conducting properties. However, as we know, PAn can exist in insulating, semiconducting, and conducting state depending on its doping state (usually H^+ doping in a strong acid). It was reported that the conductivity of PAn drops precipitately with increasing pH and it is converted to an excellent insulator in alkaline medium (MacDiarmid et al., 1985). Instead of further exploiting the most popular conducting and electroactive properties of PAn for the development of chemical and biosensing devices as it has been demonstrated in numerous reports (Wei and Ivaska, 2006), this work for the first time exploited the possibility of leveraging on the excellent insulating power of PAn to develop an EIS biosensor for miRNA expression profile analysis.

To test the feasibility of utilizing the electron insulating property of PAn as a sensitive signal generator for the EIS biosensor, a synthetic miRNA let-7b was examined at a biosensor coated with PNA CPs fully complementary to let-7b. For comparison, a totally non-complementary synthetic RNA of the same length as let-7b (control) was also tested. As seen in Fig. 2A, after a period of 60 min hybridization and subsequent 30 min incubation in the PAn deposition cocktail, a distinct difference between let-7b and the control was obtained. The EIS spectrum of the let-7b biosensor was made of a semicircle at high frequencies and a straight line with a phase angle of 45° at low frequencies (Fig. 2A trace 1). The straight line with 45° phase angle is less important because it is related to the solution diffusion process of the redox probes, known as Warburg impedance (Randles, 1947). In the case of EIS-based biosensors, characteristics of the diffusion process of the redox probes are largely independent of the biosensing processes. The semicircle in the EIS spectrum, on the other hand, is closely associated with the charge-transfer of the redox probes and its diameter is the charge-transfer resistance (R_{ct}) – a direct measure of the charge-transfer process (Randles, 1947). The large semicircle observed at the let-7b biosensor indicated that a layer of charge-transfer impeding material exists at the biosensor surface. In contrast, a straight line with a phase angle of 45° was obtained in the whole frequency range at the control (Fig. 2A trace 2), implying that R_{ct} in this case is largely insignificant. In addition a much less significant difference was erved between the control and the biosensor after hybridization and before PAn deposition (Fig. S1). Because the control is completely non-complementary to the PNA CPs, none of the miRNA strands is expected to be brought to the biosensor. On one hand, in the presence of deprotonated cysteine on the biosensor surface at pH 8.0 (hybridization buffer), nonspecific uptake of the control miRNA is effectively minimized. On the other hand, instead of a layer of anionic target miRNA strands, the protonated cysteine in the pH 3.0 PAn deposition cocktail largely retards the deposition of PAn. Therefore, the control biosensor should remain as original – the same as the blank biosensor. In addition, before the deposition of PAn, when the EIS spectrum is collected in the pH 12.0 phosphate buffer cationic $Ru(NH_3)_6^{3+/2+}$ alleviate electrostatic repulsion between now anionic miRNA and the redox probes $Ru(NH_3)_6^{3+/2+}$; and $Ru(NH_3)_6^{3+/2+}$ probes are able to approach the electrode surface closely. Therefore, there are no noticeable changes in the reversibility or R_{ct} of $Ru(NH_3)_6^{3+/2+}$ between the control and the hybridized biosensor before PAn deposition. Apparently, the large R_{ct} observed with the let-7b miRNA is closely associated with the target hybridization and PAn deposition processes – a key parameter (analytical signal) in EIS biosensors. Values of R_{ct} can be conveniently extracted from the EIS spectrum by either direct analysis of the spectrum or by fitting the spectrum to a Randle equivalent circuit (Fig. 2A inset) (Randles, 1947). The large R_{ct} indicated that a large amount of charge-transfer impeding material is present at the biosensor surface as a direct consequence of let-7b hybridization and it is possible to realize sensitive miRNA detection via the DNAzyme-catalyzed polymerization of aniline and hybridized miRNA strand-guided deposition of PAn. Upon hybridization, the target let-7b strands are brought to the biosensor surface by their complementary CPs. A subsequent incubation in the PAn deposition cocktail results in the formation of a thin PAn film alongside the hybridized miRNA strands, akin to that of HRP-catalyzed polymerization of aniline and DNA-guided deposition of PAn (Ma et al., 2004; Wang et al., 2013). Supportive evidence of the formation of the charge-transfer impeding PAn film on the biosensor surface was found in voltammetric test of the biosensor (Fig. 2B). Unlike the control which displayed the usual reversible voltammogram of Ru $(NH_3)_6^{3+/2+}$ with a peak-to-peak potential separation (ΔE_p) of 59 mV (Fig. 2B trace 2), a quasi-reversible voltammogram with smaller peak currents and a larger ΔE_p of 95 mV was obtained

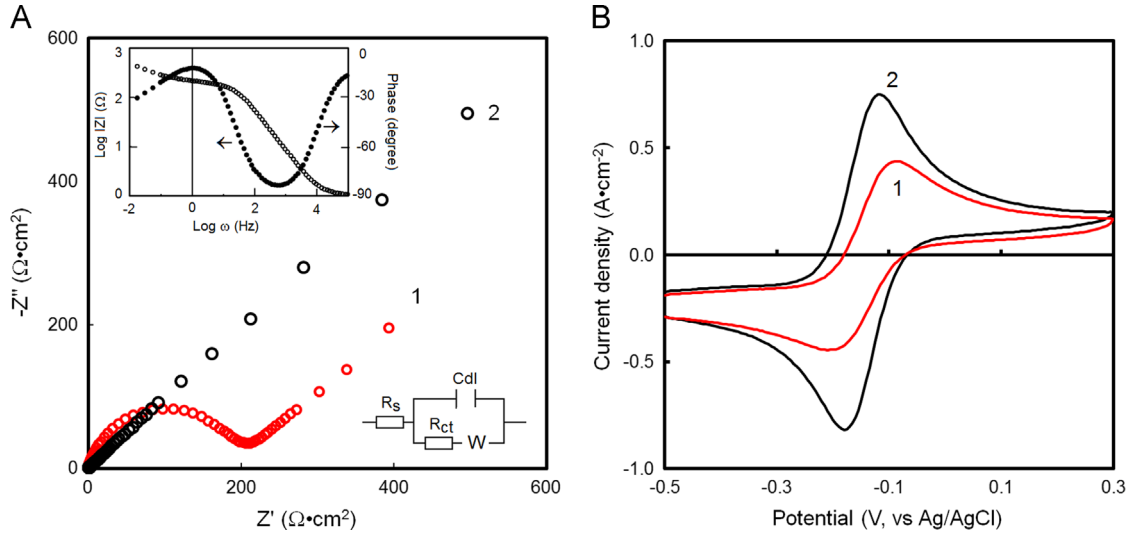

Fig. 2. (A) EIS spectra and (B) the corresponding voltammograms at 100 mV/s of a let-7b biosensor to (1) 100 fM let-7b and (2) 100 fM control RNA. 60 min hybridization at 50 °C and 30 min incubation in pH 3.0 of 0.10 M potassium phosphate containing 10 μM DNAzyme, 20 mM aniline, and 200 mM H_2O_2. Insets: (top) Bode plot of the biosensor and (bottom) Randle equivalent circuit used to fit the EIS data: R_s – solution resistance, C_{dl} – double layer capacitance, R_{ct} – charge-transfer resistance, W – Warburg impedance element.

with let-7b (Fig. 2B trace 1), again suggesting the presence of a charge-transfer impeding layer on the biosensor surface. The smaller peak currents and the larger ΔE_p are direct consequence of the resistance to charge transfer between the substrate gold electrode and $Ru(NH_3)_6^{3+/2+}$ redox probes (Sabatani and Rubimstein, 1987).

3.3. Optimization

Owing to unique attributes of miRNAs, there is little room to fine-tune the miRNA hybridization conditions. Our efforts were therefore focused on the optimization of the signal amplification (Pan deposition) process. In the case of PAn deposition, the deposition rate must be determined by one or a combination of the following: (i) mass-transport processes of aniline and H_2O_2 in solution, (ii) DNAzyme-catalyzed polymerization of aniline, which is dependent on the concentrations of DNAzyme, aniline, and H_2O_2, and (iii) miRNA-guided deposition of PAn. Under selected experimental conditions, when both the mass-transport and aniline polymerization are much faster than the PAn deposition process, the PAn deposition rate is then solely controlled by the number of the hybridized miRNA strands on the biosensor surface, and thus, by the concentration of the target miRNA. This sole miRNA-controlled process can be achieved by "speeding up" polymerization and mass transport. High mass-transport rates are obtainable when working with high concentrations of the reactants. It is critical that the polymerization of aniline should be carried out in an acidic medium with a pH value far below then pK_a of aniline ($pK_a = \sim 4.6$) (Lide, 1993), so as to create a favorable environment for the polymerization of aniline (fast polymerization rate), to effectively utilize the hybridized miRNA strands as templates to guide the deposition of PAn, and to minimize indiscriminative deposition of PAn by forming electrostatic adducts along miRNA strands between cationic aniline molecules and anionic phosphate moieties. Unfortunately, most natural enzymes are active and stable only around neutral pH values. In contrast, the chemical nature of the DNAzyme may be stable and remain active in a much wider pH range, thus well-suited for this purpose. To verify this hypothesis, we first evaluated the catalytic activity of the DNAzyme in the polymerization of aniline and the deposition of PAn. It was found that the catalytic activity toward the polymerization of aniline and deposition of PAn is strongly pH dependent, attaining its maximal activity in the pH range of 2.5–3.0 (Fig. 3A), reflected by the largest R_{ct} observed. The amount of PAn found at the biosensor surface dropped sharply to a negligible level once the solution of pH was higher than 5.0, evidently due to a much lower polymerization rate and weaker interaction between aniline and hybridized miRNA strands. No PAn deposition was detected when the pH of the PAn deposition cocktail was > 6.0. Fig. 3B shows the effect of the DNAzyme on R_{ct} of the biosensor. It was noted that as the DNAzyme concentration was increased, R_{ct} increased rapidly and almost linearly at first, but then slowly became practically independent of DNAzyme concentration at $\geq 10\ \mu M$, implying that the deposition of PAn is now solely controlled by the amount of hybridized miRNA strands on the biosensor surface. Further increase in DNAzyme resulted in excessive polymerization of aniline and an appreciable increase in R_{ct} of the control, probably due to nonspecific deposition of PAn in the presence of large excesses of PAn in the cocktail. As seen in Fig. 3B, R_{ct} of the control increased significantly from ~ 5 to $25\ \Omega\ cm^2$ in the PAn deposition cocktail containing $20\ \mu M$ DNAzyme, 20 mM aniline, and 200 mM H_2O_2, thus deteriorating the detection limit from femtomolar to picomolar levels. Therefore, 5–10 μM DNAzyme was chosen to ensure sufficiently high sensitivity and good signal-to-noise ratios. Unlike HRP which can be easily deactivated by pH and high concentrations of H_2O_2, as a small HRP-mimic the DNAzyme is expected to be very robust. Indeed, the DNAzyme was found to be much more tolerant than HPR in terms of reaction conditions. For example, it was observed that the DNAzyme remains active in a much wider range of H_2O_2 concentration from 10 μM to 400 mM, where enzyme such as HRP is quickly deactivated at H_2O_2 concentrations > 10 mM.

In addition, it was observed that a moderate amount of aniline (20 mM) produces the best result (Fig. 3C). Too low an aniline

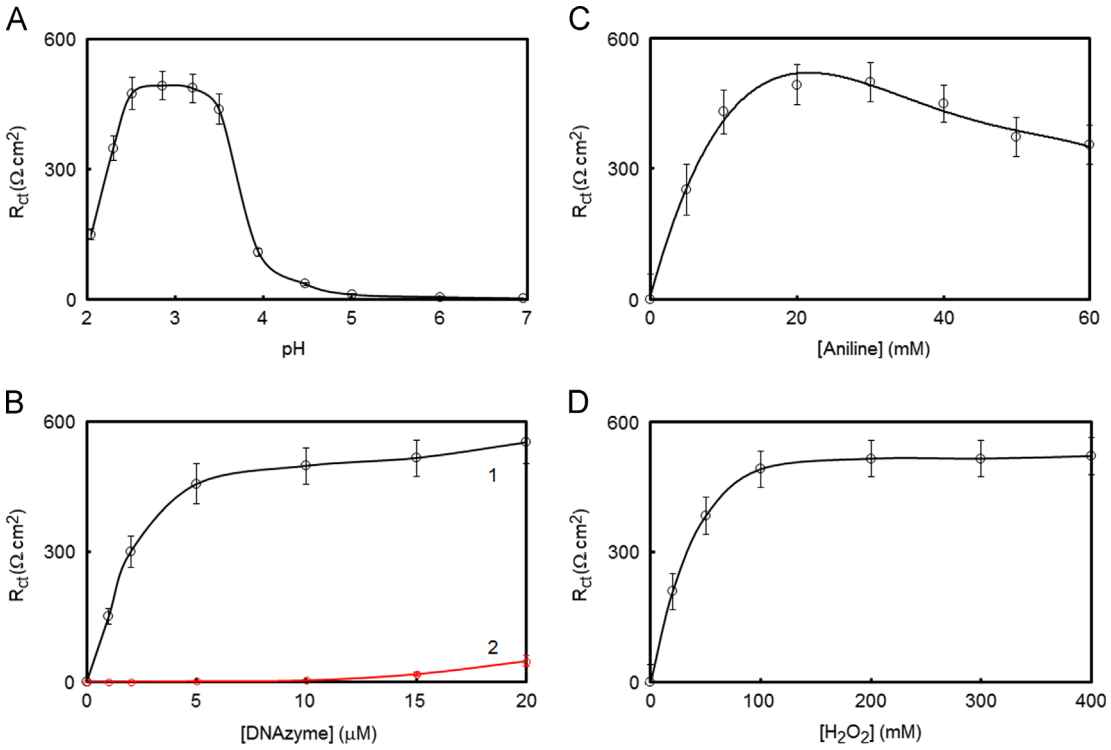

Fig. 3. Dependence of R_{ct} on (a) pH, (b) aniline, (c) DNAzyme, and (d) H_2O_2; after 60 min hybridization of 250 fM let-7b at 50 °C. Data points represented six replicates.

concentration resulted in a slow polymerization and possibly a quick depletion of aniline. Too much aniline in the PAn deposition cocktail may lead to the formation of highly soluble oligomers and low molecular weight of PAn, thus reduced the PAn deposition rate and adversely affect the sensitivity of the biosensor.

As for H_2O_2, a high enough concentration of H_2O_2 is the prerequisite for maximizing the amplification power of the DNAzyme. The high concentration of H_2O_2 ensures that there is no substantial depletion of H_2O_2 and the PAn deposition is totally independent of H_2O_2, which in turn infers that the amount of PAn deposited on the biosensor surface would scale up with the amount of the number of hybridized miRNA strands and the incubation in the PAn deposition cocktail. As shown in Fig. 3D, R_{ct} of the biosensor was maximized in the presence of $\geq$ 100 mM H_2O_2.

Since the hybridized target miRNA-guided deposition of PAn is cumulative, R_{ct} is also closely associated with the incubation time in the PAn deposition cocktail. High sensitivity is expected if the deposition of PAn is allowed to proceed for a sufficiently long period of time. To leverage on the PAn deposition for sensitivity improvement, a series of EIS tests were carried out with different incubation time in the PAn deposition cocktail. A plot of R_{ct} at different incubation time is shown in Fig. 4. In all cases, an immediate increase in R_{ct} was observed due to the formation of the charge-transfer impeding PAn films on the biosensor. At 10 and 250 fM let-7b, R_{ct} of the biosensor was found to be proportional to the incubation time throughout (Fig. 4 traces 1 and 2), suggesting that there is very little activity loss of the DNAzyme during the incubation; whereas at a much higher concentration of 5.0 pM let-7b R_{ct} of the biosensor gradually leveled off after an initial linear increasing phase (Fig. 4 trace 3). The deviations from linearity after a prolonged period of incubation is probably due to the fact that R_{ct} of the biosensor has reached such a high value that further deposition of PAn has significantly less impact on it. Eventually, R_{ct} of the biosensor may reach a steady state when the target concentration is sufficiently high and the incubation time is sufficiently long. It was found that a period of 30 min incubation is sufficient for the detection of femtomolars of miRNAs.

3.4. Analytical performance of the biosensor

Under optimized experimental conditions, standard solutions of synthetic miRNA let-7b were used to evaluate the performance of the biosensor. As shown in Fig. 5, a linear relationship between R_{ct} and let-7b concentration was observed from 1.0 fM to 5.0 pM with a regression coefficient of 0.97 and a relative standard

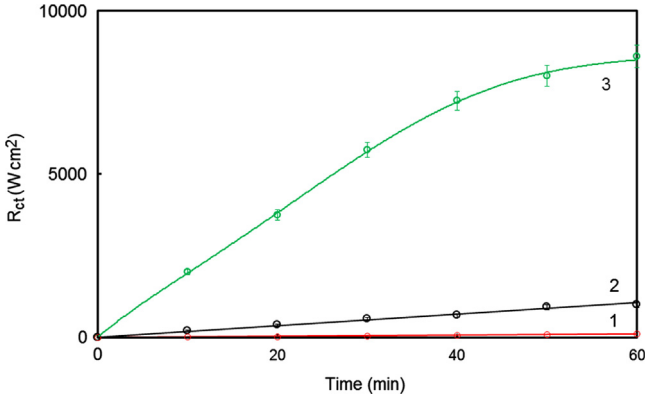

Fig. 4. Dependence of R_{ct} of (1) 10 fM, (20) 250 fM, and (3) 5.0 pM let-7b after 60 min hybridization at 50 °C on the incubation time in pH 3.0 of 0.10 M potassium phosphate containing 10 μM DNAzyme, 20 mM aniline, and 200 mM H_2O_2. Data points represented six replicates.

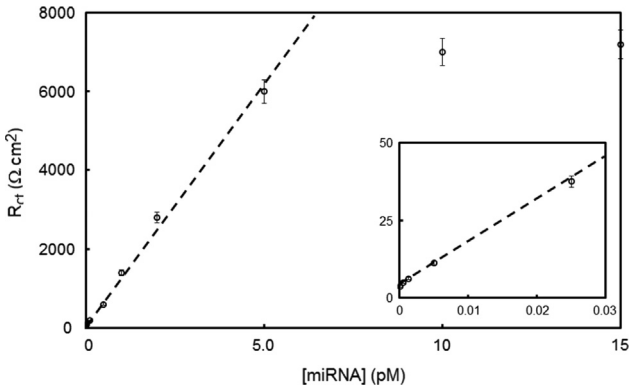

Fig. 5. Calibration curves for let-7b. 60 min hybridization at 50 °C and 30 min incubation in pH 3.0 of 0.10 M potassium phosphate containing 10 μM DNAzyme, 20 mM aniline, and 200 mM H_2O_2. Data points represented six replicates.

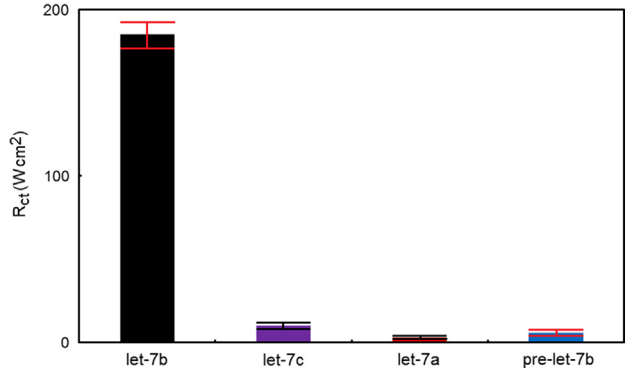

Fig. 6. EIS responses (R_{ct}) of a let-7b biosensor to 100 fM of let-7b, let-7c, let-7a, let-7e, and pre-let-7b, respectively. 60 min hybridization at 50 °C and 30 min incubation in pH 3.0 of 0.10 M potassium phosphate containing 10 μM DNAzyme, 20 mM aniline, and 200 mM H_2O_2. Data points represented six replicates.

derivation of ~14% at 100 fM. The detection limit of the biosensor was estimated to be 0.50 fM at a signal/noise ratio of 3.0 (the standard derivation in R_{ct} of six independent control biosensors was taken as the noise). As compared to previously reported EIS miRNA biosensors, the improved sensitivity is likely originated from the highly efficient polymerization and deposition of PAn. Lower detection limit was attainable with a longer hybridization and PAn deposition time.

The capability of the biosensor in selectively detecting specific miRNAs in a miRNA family was evaluated by analyzing three representative members of let-7 family, namely fully complementary (let-7b), one-base-mismatched (let-7c), and two-base-mismatched (let-7a). As seen in Fig. 6, a 95% and 99% drop in R_{ct} were observed when let-7c and let-7a were tested on the let-7b biosensor, respectively. In other words, selectivity factors of 20 and 100 were observed with one-base mismatched and two-base mismatched miRNAs, respectively. Negligible responses, indistinguishable from that of the control, were observed when miRNAs with three or more bases are mismatched. This level of mismatch discrimination ability between complementary and mismatched sequences is better than those of many hybridization-based biosensors (Sassolas et al., 2008; Tansil et al., 2005), most probably due to the much higher sequence selectivity of PNA (Nielsen, 2004). Unlike thermal amplifications employed in ligase chain reactions and qPCR, without a denaturing step the proposed biosensor is less prone to interferences from pre-miRNAs since their highly stable hairpin structures remain intact under the hybridization conditions, making miRNA regions inaccessible for hybridization to the PNA CPs. A selectivity factor of ~40 was

obtained when equal molars of let-7b and pre-let-7b were analyzed at the let-7b biosensor.

3.5. Sample analysis

Apart from its high sensitivity, the freedom from miRNA labeling and thermal amplification greatly improve the suitability of the proposed biosensor in direct profiling miRNAs with minimal sample preparation. Attempts were therefore made in employing the biosensor for analyzing miRNAs in total RNA extract from cultured cancer cells and blood. The same total RNA samples were also analyzed by qPCR. Consistent results were obtained with the biosensor and qPCR on the same sample. Statistically, no significant difference was observed between the proposed biosensor and qPCR. Due to its high sensitivity, only nanograms total RNA was needed for a successful detection of miRNA with the biosensor. Without a sample preparation step, miRNA expression can be performed within 120 min.

As compared to other miRNA detection techniques, the much-simplified label-free approach and isothermal amplification process via the catalyzed polymerization and deposition of PAn makes the proposed biosensor particularly attractive for routine miRNA analysis. The freedom from tedious total RNA sample preparation, chemical/biological ligation, and PCR amplification will significantly improve the suitability in direct profiling miRNAs with minimal or no sample pretreatment. This work only serves as a proof-of-concept through rather laborious manual operation. Nonetheless, the much simplified procedure suggests that the throughput can also be significantly improved by upgrading the manual operation to a microfluidic cartridge and by constructing high-density sensor arrays using the standard microfabrication technology and the complementary metal-oxide semiconductor technology. However, because of the unique attributes of miRNAs, such as their short lengths, inherently different melting temperatures, and high similarities among members of a miRNA family, great care must be taken when profiling multiple miRNAs simultaneously since there is very little room to fine-tune the hybridization conditions for all miRNAs.

4. Conclusion

The present study demonstrated a biosensor for miRNA expression profiling. The combination of the charge neutral PNA CPs and the guided deposition of PAn leads the unique amplified label-free EIS biosensor for miRNAs. Without the need for miRNA labeling, the assay procedure is greatly simplified. The adoption of the guided deposition of PAn provides a convenient means of sensitivity improvement. Being capable of analyzing real-world samples without thermal cycling and with minimal sample preparation, the proposed biosensor is an attractive candidate for the development of a simple and sensitive miRNA expression profiling tool for uses at point-of-care.

Acknowledgments

The work is supported by A*STAR through the A*STAR-ANR Program (Grant No. 1222703071).

Appendix A. Supporting information

Supplementary data associated with this article can be found in the online version at http://dx.doi.org/10.1016/j.bios.2014.04.023.

References

Briones, C., Mateo-Marti, E., Gomez-Rodriguez, C., Parro, V., Roman, E., Martín-Gago, J.A., 2004. Phys. Rev. Lett. 93, 20810.
Dodgson, B.J., Mazouchi, A.D., Wegman, W., Gradinaru, C.C., Krylov, S.N., 2012. Anal. Chem. 84, 5470–5474.
Driskell, J.D., Tripp, R.A, 2010. Chem. Commun. 46, 3298–3300.
Duan, D.M., Zheng, K.X., Shen, Y., Cao, R., Jiang, L., Lu, Z.X., Yan, X.Y., Li, J., 2011. Nucleic Acids Res. 39, e154.
Gao, Z.Q., Deng, H.M., Shen, W., Ren, Y.Q., 2013. Anal. Chem. 85, 1624–1630.
Husale, S., Persson, H.H.J., Sahin, O., 2009. Nature 462, 24–31.
Johnson, B.N., Mutharasan, R, 2012. Anal. Chem. 84, 10426–10436.
Lide, D.R., 1993. Handbook of Chemistry and PhysicsCRC Press, Boca, Raton, FL, pp. D159–D161.
Ma, Y., Zhang, J., Zhang, G., He, H., 2004. J. Am. Chem. Soc. 126, 7097–7101.
MacDiarmid, A.G., Chiang, J.C., Halpern, M., Huang, W.S., Mu, S.L., Somasiri, N.L.D., Wu, W., Yangier, S.I., 1985. Mol. Cryst. Liq. Cryst. 121, 173–180.
Nielsen, P.E. (Ed.), 2004. Peptide Nucleic Acids-Protocol and Applications. Horizon Bioscience, Norfolk.
Peng, Y.F., Gao, Z.Q., 2011. Anal. Chem. 83, 820–827.
Randles, J.E.B., 1947. Discuss. Faraday Soc. 1, 11–13.
Sabatani, E., Rubimstein, I., 1987. J. Phys. Chem. 91, 8663–8669.
Sassolas, A., Leca-Bouvier, B.D., Blum, L.J., 2008. Chem. Rev. 108, 109–139.
Shen, Y., Zheng, K.X., Duan, D.M., Jiang, L., Li, J., 2012. Anal. Chem. 84, 6361–6365.
Shen, W., Deng, H.M., Ren, Y.Q., Gao, Z.Q., 2013a. Chem. Commun. 49, 4959–4961.
Shen, W., Deng, H.M., Ren, Y.Q., Gao, Z.Q., 2013b. Biosens. Bioelectron. 44, 171–176.
Tansil, N.C, Xie, H., Xie, F., 2005. Anal. Chem. 77, 126–134.
Travascio, P., Li, Y., Sen, D., 1998. Chem. Biol. 5, 505–517.
Wang, Z.G., Zhan, P.F., Ding, B.Q., 2013. ACS Nano 7, 1591–1598.
Wegman, D.W., Krylov, S.N., 2011. Angew. Chem. Int. Edit. 50, 10335–10339.
Wei, D., Ivaska, A., 2006. Chem. Anal. 51, 839–852.
Yin, B.C., Liu, Y.Q., Ye, B.C., 2012. J. Am. Chem. Soc. 134, 5064–5067.
Zhang, Y., Li, Z., Cheng, Y., Lv, X., 2009. Chem. Commun., 3172–3174.